Universiteit Leiden

Master Computer Science

Applying Counterfactual Explanations and Multivariate Forecasting to Medical Prediction Tasks

Name:	Tomke Meyer
Student ID:	s2231086
Date:	dd/mm/2025
Specialisation:	Bioinformatics
1st supervisor:	Jan van Rijn
2nd supervisor:	Panagiotis Papapetrou

Master's Thesis in Computer Science

Leiden Institute of Advanced Computer Science (LIACS)
Leiden University
Niels Bohrweg 1
2333 CA Leiden
The Netherlands

Abstract

Contents

1 Introduction

The goal of this thesis is to gain insights into the application of multivariate forecasting and counterfactual explanations to medical prediction tasks. [**TODO:** more thesis introduction, what is the goal, what is the motivation]
The global population is both growing and ageing, which is resulting in a rise in chronic diseases. This is resulting in a demand for more efficient, personalised, and proactive healthcare solutions [HSL+23]. Previously, treatment was only provided once symptoms had appeared, and treatment plans were very general. Nowadays, this approach is no longer sufficient, as patients are in need of a more personalised approach to their care. Technological advancements in the field of healthcare have had a significant impact on healthcare providers and patients, with statistical methods being used to predict outcomes. This approach struggles with the complex nature of clinical, demographic and molecular factors that influence the disease progression, leading to Machine Learning (ML), Deep Learning (DL), Artificial Intelligence (AI), and Big Data Analytics becoming increasingly popular fields within the medical and health science domains [ASFWHY+25]. Recent healthcare has been characterised by an increased need for data-driven approaches, with the care process being driven by the flow of data between patients and doctors, and the sharing of decisions, instructions and information amongst care providers. The role that data and information play in decision making and provision of healthcare, has only increased with the growing digitisation of healthcare. This results in great amounts of data, which enables the implementation of advanced analytical methods, including ML and AI, to derive valuable and actionable insights. These insights are essential in supporting decision-making processes, ensuring high quality patient care, responding to real-time situations and ultimately reducing mortality. Especially ML becomes more and more relevant in healthcare applications, including predictive analysis, treatment optimisation, and patient monitoring [MPS19]. ML algorithms can potentially be used to improve diagnostic accuracy, as well as support early disease detection and prediction. Other applications include, analysing medical imaging data, such as X-rays and MRIs, to detect signs of cancer or neurological disorders, which allows for early diagnosis, as well as a personalised treatment plan for each patient. These uses show the potential ML has for both research and clinical trials, and support the improvement of healthcare overall [RNZ17], [JHS+22].

Time series analysis uses an ordered sequence of data points recorded over time, usually at regular intervals, to understand patterns, trends, and relationships within the data over time. This time series data also allows for forecasting or predicting future values, based on historical observations. Time series forecasting plays a crucial role in a number of different applications. Some applications include its usage in finance, for predicting stock prices and market trends [MSG14], in meteorology for weather and climate forecasting [KS20], in transportation, for effective traffic flow forecasting [LBF13] and especially recently in healthcare. In healthcare, time series forecasting is increasingly relevant, as patient data such as heart rate, blood pressure, glucose levels, and laboratory results are being collected continuously or in regular intervals. Precise forecasting of these medical time series can allow for early detection of negative outcomes, support the personalisation of treatment plans, and optimise healthcare management overall [KCS+20], [JPS+16].

[**TODO:** Extend, add citations] Generally, time series forecasting consists of finding tem-

poral dependencies and trends in the data. Depending on the nature of the time series, such as for example linear or non-linear, stationary or non-stationary, and univariate or multivariate, requires different forecasting methods. These different forecasting methods can be categorised into three subgroups, statistical models, such as ARIMA and ETS, ML models, such as Linear Regression and SVRs, and DL models, such as RNNs, LSTMs, GRUs as well as transformer-based models Autoformer or DLinear.
Especially the latter models have shown promising results in recent years, achieving very accurate predictions. Despite these recent developments, many deep-learning based forecasting systems are considered "black-box"-models, as it is challenging to interpret and understand both the modelling process and the forecasting outcome. This is particularly problematic in healthcare applications, where especially interpretability is very important, as clinicians need to understand the reasoning behind the predictions to make informed decisions. One approach to tackle this problem is working with counterfactual explanations, which aim to identify small changes in the input variables needed to change a model's forecast to a more desirable outcome.
In healthcare, time series forecasting has been applied to a number of different tasks, especially the analysis of electronic health records (EHRs). These contain information about a patient's health over time, allowing predictions about the disease progression, treatment efficacy or patient mortality. For example, forecasting glucose levels in diabetic patients or predicting heart failure with preserved ejection fraction (HFpEF) can aid early interventions and optimise treatment plans.
Traditional time series forecasting focuses mainly on predicting future values given historical observations, but modifying past values is not feasible in real-world settings, especially in healthcare applications. Instead, a more practical approach is to explore how changing exogenous variables during the forecast horizon could lead to a desired outcome. This approach allows continuous monitoring of patients, making it possible to dynamically adjust treatment plans to lead towards more optimal results.

1.1 Diabetes

Diabetes is one of the most prevalent chronic diseases in the world, with it being a leading cause of death and disability. According, to the World Health Organisation (WHO), around 830 million people worldwide suffer from diabetes, and it is the direct cause of 1.5 million deaths a year. Nowadays, it affects around 14% of adults, this number has doubled since 1990, making it a major public health problem. Diabetes is characterised by elevated levels of blood glucose, which over time seriously damages the heart, blood vessels, eyes, kidneys and nerves. Type 2 diabetes is much more common and occurs when the body either becomes resistant to insulin or does not make enough insulin. It usually has a later onset and its development can be attributed to factors such as being overweight, not getting enough exercise and genetic. Type 1 Diabetes is a chronic condition, where the pancreas only produces little to no insulin by itself. It is caused by the autoimmune destruction of pancreatic β-cells and affects 5-10% of the diabetes patients [Dia], [ame25]. For patients with conditions such as type 1 diabetes mellitus (T1DM), closely tracking their glucose levels is a necessity. To reduce the risk of complications such as hyperglycaemia or hypoglycaemia, these patients rely on continuous glucose monitoring (CGM) devices and automated insulin delivery. Using machine learning (ML) to model CGM, can help to gain a better understanding of predicting abnormal glucose events

and help with insulin dosage planning. By also incorporating variables such as insulin intake, carbohydrate consumption, and physical activity, a predictive model can allow timely interventions through the generation of actionable recommendations for patients or healthcare providers. This allows for more dynamic treatment based on these forecasted expected glucose trends, which can reduce the long-term risk of diabetes-related complications [Com25].

1.2 Heart failure with preserved ejection fraction

Heart failure with preserved ejection fraction (HFpEF) is a prevalent and severe cardiovascular condition [BP11]. Heart failure (HF) is classified based on the left ventricular ejection fraction (LVEF) and can be split into three subcategories. Heart failure with reduced ejection fraction (HFrEF) with LVEF $\leq$40%, heart failure with mildly reduced ejection fraction (HFmrEF) with LVEF = 41-49%, and heart failure with preserved ejection fraction (HFpEF) with LVEF $\geq$50% [MMA+21]. Studies have shown that the mortality within one year is around 29%, [OHH+06], [SBA+24], with increased mortality for patients with previous heart failure hospitalisations and other comorbidities [MGL+20]. This makes HFpEF a very serious condition, where early diagnosis is key. So another possible application of medical time series forecasting could be to try identifying early warning signs of heart failure or more specific HFpEF to suggest either lifestyle or treatment changes. Using the vital signs, as for example the heart rate and blood pressure, of a patient as well as other factors like gender and possible comorbidities, allows specific and personal monitoring of disease progression. This way, early warning signs of worsening heart condition can be identified and personalised modifications to lifestyle or medication can be suggested. Such proactive monitoring can help reduce hospital readmissions and improve patient outcomes.

1.3 Counterfactual Explanations

Counterfactual explanations (CE) are an emerging technique with the potential to improve the interpretability and explainability of ML models. The objective is to identify minimal changes to the input features that would result in a different, and typically more desirable, outcome. More specifically, they provide information such as if an input data point would be X' instead of X, then the trained ML models prediction would be Y' instead of Y, assuming outcome Y' would be more favourable [VDH21]. So counterfactuals are a type of explanation method in ML, that might help users to understand the model predictions and decisions better. This is supported by counterfactual explanations being actionable, since they suggest specific changes to alter the outcome, and intuitive for humans, since they align with human reasoning about cause and effect. Often CEs are also model-agnostic, meaning they can be applied to a variety of black-box models [Gui24]. A more specific example application of counterfactuals would be a suggestion that slightly reducing a patients systolic blood pressure could have led to a prediction of a lower cardiovascular risk. So these kind of insight can not only help clinicians understand a models decisions better, but also provide help for intervention and treatment planning.

1.4 Related Work

[**TODO:** check, add citations, rewrite]

1.4.1 Related Forecasting Models

Recent research has explored various deep learning (DL) models for time series forecasting, including recurrent neural network (RNN)-based models such as gated recurrent units (GRU) and long short-term memory (LSTM), as well as attention-based architectures like transformers. Transformer-based models, including Autoformer and Informer, have demonstrated strong performance in both univariate and multivariate forecasting tasks by capturing long-range dependencies more effectively than traditional RNN approaches. In the clinical domain, deep learning models have been applied extensively to glucose forecasting. For instance, Deep Multi-Output Forecasting [FAJ+18] introduced a multi-step forecasting framework that explicitly models the distribution of future glucose values over a prediction horizon using a multi-output deep architecture. Similarly, WaveNet has been adapted for glucose forecasting by leveraging dilated convolutional neural networks (CNNs) to model long-term dependencies [ZLH+18]. In addition, transfer learning techniques have been employed to enhance predictive performance by fine-tuning pre-trained models on patient-specific data while incorporating exogenous covariates such as insulin dosage and carbohydrate intake [MB20].

Beyond predictive performance, explainability remains a critical challenge in deep learning-based forecasting models. Traditional statistical models, such as ARIMAX and VARIMAX, are able to quantify relationships between exogenous factors and the target variable, but their forecasting accuracy is often outperformed by DL approaches. Recent research has focused on integrating explainability into forecasting models to combine the strengths of both interpretability and predictive performance. For example, NBEATSx extends the NBEATS framework by incorporating exogenous variables into its deep architecture, enabling a more structured decomposition of trend and seasonality. However, its interpretability remains static and does not fully capture the dynamic nature of forecasting outcomes.

To address the need for explainability, counterfactual explanations have gained traction in time series analysis. Initial efforts focused on time series classification, where counterfactuals were generated through instance-based modifications and gradient-based perturbations [AALC21]. This was done by introducing a framework for generating counterfactual explanations for multivariate time series classification, identifying minimal input modifications needed to alter the model's decision, providing interpretability for high-dimensional time series models.

More recently, counterfactual explanations have been extended to time series forecasting. ForecastCF [WMSP23] proposed a deep learning-based method for generating counterfactuals in time series forecasting by identifying minimal input changes required to achieve desired prediction outcomes. Building on this, COMET [WSMP24] extended counterfactual explanations to multivariate time series forecasting, focusing on modifying exogenous variables (e.g., insulin, carbohydrates, and exercise) to generate actionable recommendations for glucose management.

In addition to counterfactual forecasting, diagnostic tools like TimeTuner [HSYZ23] have been developed to analyse how time representations influence forecasting models. By employing counterfactual explanations, TimeTuner enables the evaluation of multivariate time series representations and their impact on model predictions.

Despite these advances, counterfactual explanations for multivariate time series analysis remain an emerging research area. While existing methods demonstrate the feasibility of generating counterfactuals for univariate forecasts, their generalisation to multivariate forecasting and real-world clinical applications remains limited. This work aims to extend on these existing methods by integrating counterfactual reasoning with multivariate forecasting models, focusing on modifying exogenous variables within the prediction horizon to provide actionable and interpretable interventions.

1.4.2 Related Work in Glucose Forecasting

Forecasting physiological indicators such as blood glucose levels, is crucial for managing diabetes. Time series forecasting and model explainability are becoming increasingly important in this field of medical prediction tasks, as in many others. Recent contributions to this area of research highlight the growing use of multivariate machine learning models to improve predictive accuracy and personalisation. This shows the growing need for interpretable and actionable insights, which aligns closely with the goals of this thesis.
Recent research highlights the growing development of multivariate and deep learning-based models for predicting glucose levels. For example, Kalita and Mirza [KM25] proposed a model that combines multi-head attention layers with neural basis expansion networks, capturing complex temporal and cross-feature dependencies in glucose data. Similarly, Benaida et al. [BAI25] demonstrated the effectiveness of deep learning architectures for both single- and multi-step glucose forecasting, emphasising the importance of longer-term prediction capabilities in real-world applications. These multivariate models are consistent with the focus of this thesis on leveraging multiple signals, such as past glucose levels, physiological parameters, and contextual variables, for accurate forecasting.
Personalisation has emerged as a key factor in clinical forecasting settings, as patient diversity affects model performance. Shen and Kleinberg [SK25a] addressed this issue by using incrementally retrained LSTM networks that adapt to each individual's glucose dynamics. This improves performance, even when the CGM data is limited. Lara-Abelenda et al. [LCP+25] introduced large language models (LLMs) to model personal glucose trends, highlighting the capacity of foundation models to generalise across individuals while retaining patient-specific nuances. These methods emphasise the importance of adaptive and context-aware forecasting.
Several works have also incorporated physiological signals beyond glucose levels to support multivariate forecasting. For example, Giancotti et al. [GBV+24] explored the utility of heart rate as a predictor of forecasting glucose levels in patients with type 1 diabetes, which demonstrates that multimodal data can significantly enhance predictive accuracy. Similarly, Rodríguez-Rodríguez et al. [RCR23] utilised data, such as physical activity and diet logs, to enable more holistic and personalised glycaemic forecasting.
Interpretability remains a major challenge for deep learning-based forecasting models, especially in critical fields such as medicine. In response to this, Sun and Kosmas [SK25b] combined Bayesian forecasting with expert medical knowledge to model CGM values in type 2 diabetes patients. Their framework improves both uncertainty quantification and clinician interpretability, which is an essential consideration in healthcare AI. The need for model transparency directly motivates the use of counterfactual explanations to improve the explainability and actionability of predictive models in medical applications. While many current studies emphasise predictive accuracy, fewer address how predictions can

be explained and acted upon by clinicians or patients.
Taken together, these studies reflect a shift towards data-driven, multivariate, and personalised models for medical forecasting. However, there remains a clear gap in integrating these powerful models with robust, interpretable explanations. This thesis aims to bridge this gap by combining multivariate forecasting approaches with counterfactual reasoning, to provide accurate predictions and actionable, understandable explanations, which are essential components for supporting medical decision-making and patient self-management.

1.4.3 Related Work in Mortality Prediction of Patients with HFpEF

Heart Failure with Preserved Ejection Fraction (HFpEF) is a complex and heterogeneous condition, characterised by diagnostic and prognostic uncertainty. This makes it a compelling use case for machine learning (ML) in clinical decision support. Recent research has applied various ML techniques to improve diagnosis, predict outcomes such as hospitalisation and mortality, and guide individualised management strategies. These efforts emphasise the increasing relevance of multivariate forecasting and the growing demand for explainable models, which are central to the objectives of this thesis.
A significant amount of research has focused on prognostic modelling using structured clinical data. For example, Hu et al. [HMH+25] developed and validated a machine learning model to predict the risk of readmission within one year for HFpEF patients, demonstrating the utility of routinely collected electronic health records (EHRs) in anticipating adverse outcomes. Similarly, McDowell et al. [MKT+24] constructed models for predicting both mortality and morbidity in HFpEF patients, showing that complex risk factors, including comorbidities and laboratory values, can be effectively integrated into predictive models. These studies emphasise the importance of leveraging multivariate data sources to forecast long-term patient outcomes.
Short-term outcome prediction has also been explored, particularly in the context of the early identification of high-risk patients. The study "Predicting 30-Day and 1-Year Mortality in HFpEF" [SBA+24] used machine learning to predict short-term mortality, which is essential for planning acute care. Other models have focused on hospitalisation prediction, using historical patient trajectories to anticipate future events. These forecasting tasks not only require accurate time series modelling but also benefit from interpretability to inform clinical decisions.
The diagnosis of HFpEF remains a challenging area due to its symptomatic overlap with other heart failure subtypes. Kavas et al. [KBKB23] developed an ML-based decision support system using photoplethysmography (PPG) signals to differentiate between HFpEF and HFrEF (Heart Failure with reserverd Ejection Fracion), demonstrating the potential of non-invasive, sensor-based diagnostics. Liao and Hung [LH+24] further extended this approach by incorporating data from a wearable patch device to enhance diagnostic precision. These works highlight the growing role of physiological signal data in heart failure classification, which directly supports multivariate modelling approaches by introducing continuous and high-frequency signals into prediction tasks.
Genomic and molecular data have also been used to support precision medicine approaches in HFpEF. Zhou et al. [ZGW+21] utilised gene expression profiles to build ML models capable of risk stratification in HFpEF patients, adding a layer of biological interpretability to purely clinical models. Although these models are powerful, they are often perceived as "black boxes," emphasising the need for explainability techniques such as counterfactual

explanations to bridge the gap between model prediction and clinical insight.
Across these studies, however, the challenge of model transparency and interpretability remains largely unaddressed. Most existing models prioritise predictive performance without offering sufficient explanations for individual predictions, which is a critical issue in medical contexts where understanding why a prediction was made is often as important as the prediction itself. This thesis aims to bridge this gap by integrating counterfactual reasoning into multivariate forecasting models, offering clinicians not just a forecast, but a clear explanation of the factors driving the prediction and the minimal changes that could alter an adverse outcome.
In summary, the current research in HFpEF prediction demonstrates the power of machine learning to handle complex, multivariate data across diagnostic and prognostic applications. However, a lack of interpretability limits clinical adoption. This thesis tries to contribute to the field by combining accurate time series forecasting with interpretable, counterfactual explanations, thereby supporting more transparent and actionable decision-making in heart failure care.

1.5 Main Contributions

[**TODO:** Check, rewrite?] Time series forecasting can be quite useful in healthcare by predicting how well a treatment works or predicting the risk of complications, relapse or mortality. Recent studies, such as COMET [WSMP24], have been focusing on counterfactuals in time series forecasting, but these methods work by altering historical observations. Our work aims to bridge this gap by developing a counterfactual forecasting mechanism that identifies optimal changes in exogenous variables during the forecast horizon to achieve desirable outcomes. More specifically, we propose a method that learns the relationship between the forecasted targets and exogenous variables, which leads to a more effective and interpretable decision-making in healthcare.
The main contributions of this thesis can be summarised as follows:

- We propose a new model for counterfactual time series forecasting to achieve a desired constrained forecast by modifying exogenous variables within the forecast horizon.
- We incorporate existing forecasting models, such as SARIMAX, OLS, GRU and NBEATSx, for learning the relationship between exogenous variables and a target variable to ensure actionable and interpretable predictions.
- We evaluate the models on two applications in healthcare, specifically for glucose level prediction and HFpEF management, demonstrating the practical utility of our approach.

2 Methodology

2.1 Problem Formulation

1) Let $\boldsymbol{X} := (\boldsymbol{x}_i)_{i\in\{1,\dots,n\}}$ be a time series of length n (*back horizon*), with each $x_i \in \mathbb{R}^{m+1}$ composed of the target variable $y_i \in \mathbb{R}$ and the exogenous variables

$$z_i = \begin{pmatrix} z_{1,i} \\ \vdots \\ z_{m,i} \end{pmatrix} \in \mathbb{R}^m.$$

Then $\boldsymbol{X}$ can be denoted as the combined matrix of the target vector $\boldsymbol{y} \in \mathbb{R}^{1\times n}$ and the exogenous matrix $\boldsymbol{Z} \in \mathbb{R}^{m\times n}$:

$$\boldsymbol{X} = \begin{pmatrix} \boldsymbol{y} \\ \boldsymbol{Z} \end{pmatrix} := \begin{pmatrix} y_1 & \dots & y_n \\ z_{1,1} & \dots & z_{1,n} \\ \vdots & \ddots & \vdots \\ z_{m,1} & \dots & z_{m,n} \end{pmatrix}.$$

The relationship between $\boldsymbol{y}$ and $\boldsymbol{Z}$ can be described by the function:

$$r : \mathbb{R}^{m\times n} \to \mathbb{R}^{1\times n}$$

which calculates the target vector from the exogenous matrix:

$$r(\boldsymbol{Z}) = \boldsymbol{y}.$$

2) Given a time series forecasting model f that predicts the next t values (*forecasting horizon*) of $\boldsymbol{X}$, we define the forecast as:

$$f(\boldsymbol{X}) = \boldsymbol{X'} := (x_{n+i})_{i\in\{1,\dots,t\}}.$$

Additionally, consider a lower and upper bound set of constraints for each time step in the forecasting horizon, denoted as:

$$\boldsymbol{\alpha} = (\alpha_{n+i})_{i\in\{1,\dots,t\}}, \boldsymbol{\beta} = (\beta_{n+i})_{i\in\{1,\dots,t\}}.$$

The objective is to generate a counterfactual time series sample $\boldsymbol{Z}^*$, such that $\boldsymbol{y}^* = r(\boldsymbol{Z}^*)$ satisfies the given bounds:

$$\alpha_i \le y_i^* \le \beta_i, \forall y_i^* \in \boldsymbol{y}^*, i \in \{n+1, \dots, n+t\}.$$

Summarized research objective: Given a target vector $\boldsymbol{y}$ affected by the exogenous matrix $\boldsymbol{Z}$, a forecast horizon t, the original forecasted vector $\boldsymbol{y'}$ and the original forecasted exogenous matrix $\boldsymbol{Z'}$, the goal is to modify $\boldsymbol{Z'}$ to $\boldsymbol{Z}^*$ such that the corresponding target vector $\boldsymbol{y}^*$ is within constraints $\boldsymbol{\alpha}$ and $\boldsymbol{\beta}$.

2.2 Algorithm

[**TODO:** update, check] The developed algorithm takes as input time series data, split into the target variable and the exogenous variables. Additionally a number of parameters are defined, such as the learning rate, the desired bounds, the clipping range, the maximum number of iterations as well as different forecasting and regression models. The output is then the desired exogenous counterfactuals with the desired target outcome. First the multivariate forecasting is done, resulting in a target and exogenous variables that are then used for the counterfactual generation. The counterfactual generation starts with selecting test samples to generate the necessary bounds.After initializing the loss function, the counterfactuals are generated using gradient perturbation with an Adam optimizer. The gradient perturbation includes two different constraints, a clipping constraint that ensures that the exogenous variables are within a given constraint range and a historical constraint, to ensure that the counterfactuals are more similar to historical input values. Algorithm 1 shows a pseudocode of the algorithm described above.

2.2.1 Constraints

Algorithm 1 Counterfactual Hybrid Forecasting

Input: Time series data: target t, exogonous variables E, learning rate η, desired bounds (α, β), clipping range (ρ, ϕ), max iterations max_iter, differentiable forecaster $f(\cdot)$ differentiable regressor $r(\cdot)$, w, $\mathcal{G}$
Output: Counterfactual E' with desired outcome t'
$(t^*, E^*) \leftarrow (t, E)$
$(\hat{t}^*, \hat{E}^*) \leftarrow f(t^*, E^*)$
$\mathcal{S} \leftarrow$ SelectTestSamples
$(\alpha, \beta) \leftarrow$ GenerateBounds$(\mathcal{S})$
$loss \leftarrow L((t^*, E^*), \alpha, \beta, (t, E))$
$t \leftarrow 0$
while $(\hat{t}^* > \beta$ **or** $\hat{t}^* < \alpha) \wedge (t <$ max_iter$)$ **do**
    $\hat{E}^* \leftarrow$ AdamOptimize$(\hat{E}^*, loss, \eta)$
    $\hat{E}^* \leftarrow$ Clip$(\hat{E}^*, \rho, \phi)$
    $\hat{t}^* \leftarrow r(\hat{E}^*)$
    $C \leftarrow$ HistValueConstraint$(\hat{E}^*, \mathcal{G})$
    loss $\leftarrow L(\hat{E}^*, w, \alpha, \beta, X^*)$
    $t \leftarrow t + 1$
end while
$(t', E') \leftarrow (t, E)$
return (t', E')

2.3 Data

While the proposed model has broad applicability across domains beyond healthcare, this study focuses exclusively on medical use cases. In particular, we investigate the models usefulness in optimizing treatment plans for two conditions: type 1 diabetes and heart failure with preserved ejection fraction (HFpEF). The datasets used in these experiments

contain physiological measurements and treatment-related variables, allowing for personalized forecasts and counterfactual intervention generation. To prepare the data for modelling, several preprocessing steps have been applied. First, the data is split into training, validation and test sets and normalized using min-max scaling to ensure stable and consistent model training. The data is then separated into target variables and exogenous inputs. Then, a sequence generator is employed to segment the time series into overlapping windows comprising a back horizon (historical input) and a prediction horizon (target output). This is done both for the target variable alone and for sequences that include both the target and exogenous features. Any sequences containing missing values are discarded to ensure data integrity.

2.3.1 SimGlucose

The SimGlucose dataset is generated using the FDA-approved UVA/PADOVA type 1 diabetes simulator [Xie18], a Python-based tool that models the physiological responses of individuals with type 1 diabetes. The simulator includes 30 virtual patients, comprising of 10 adults, 10 adolescents, and 10 children and produces continuous glucose monitoring (CGM) measurements along with insulin dosages and carbohydrate intake events. The dataset is generated with a predefined CGM sampling frequency and insulin pump settings based on the algorithm developed in [MML+14]. For this study, simulated data was generated for ten adult patients over a one-week period. The blood glucose (BG) levels serve as the primary target variable, while the insulin dosage and carbohydrate intake are used as exogenous variables influencing the glucose levels. After generation, the data undergoes preprocessing steps as described above to prepare it for the forecasting and counterfactual generation. An example of the generated data is shown in Figure 1. In this example, BG denotes blood glucose levels, CHO indicates carbohydrate intake, and Insulin reflects the administered dosage. The risk index illustrates periods of hyperglycaemic or hypoglycaemic risk. The green band in the BG trace highlights the target glucose range (70–180 mg/dL), while red regions denote values that fall outside this range, corresponding to hypo- or hyperglycaemia.

2.3.2 OhioT1DM:

The OhioT1DM dataset [MB20] contains real-world glucose monitoring data collected from 12 individuals with type 1 diabetes over an eight-week period by Ohio University. Following prior research [CHN+21], [WSMP24], we extracted the most clinically relevant features for forecasting: continuous glucose monitoring (CGM) measurements, basal insulin, bolus insulin, carbohydrate intake, and physical activity. Compared to the SimGlucose dataset, OhioT1DM includes a more varied set of exogenous variables, particularly basal and bolus insulin administration, dietary intake, and physical activity data. As a real-world dataset, it presents additional challenges such as missing values and irregular sampling intervals. These are addressed using interpolation and resampling techniques to ensure consistency in the input sequences. The inclusion of diverse exogenous variables enables the development of more nuanced counterfactual interventions and supports improved forecasting performance. Figure 2 illustrates a 24-hour time window for one patient, showing the temporal relationship between glucose levels, insulin administration,

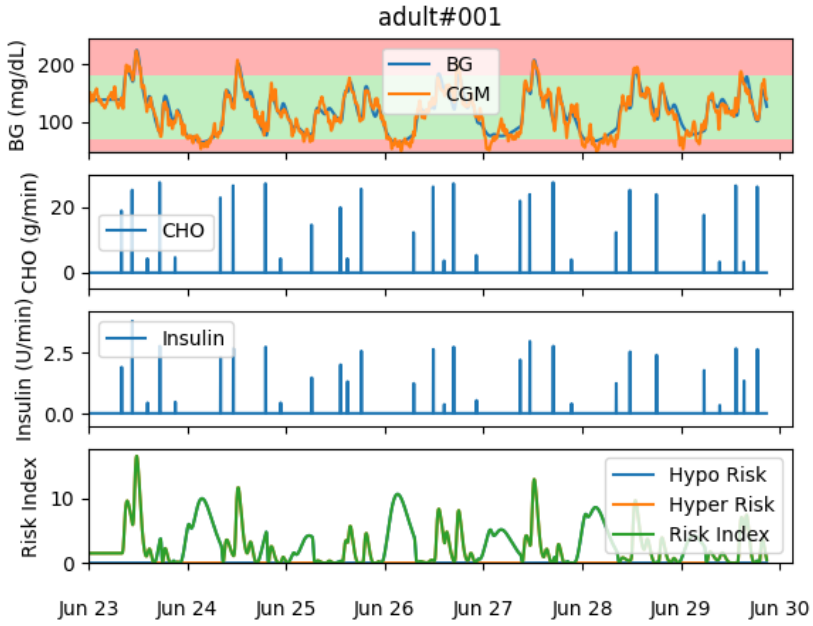

Figure 1: Simulation of an adult patient over the span of one week.

and carbohydrate consumption. The blue dotted line represents CGM-based blood glucose levels, while the black line represents the basal insulin, reflecting its slow-acting, sustained delivery throughout the day. Orange dots indicate the amount of bolus insulin, while small blue boxes indicate meals. Spikes in blood glucose often correspond to meal times (carbohydrate intake), followed by bolus insulin doses that aim to bring glucose back into the target range. This visualization exemplifies the complex dynamics and temporal dependencies that the model must capture to enable accurate and personalized glucose forecasting.

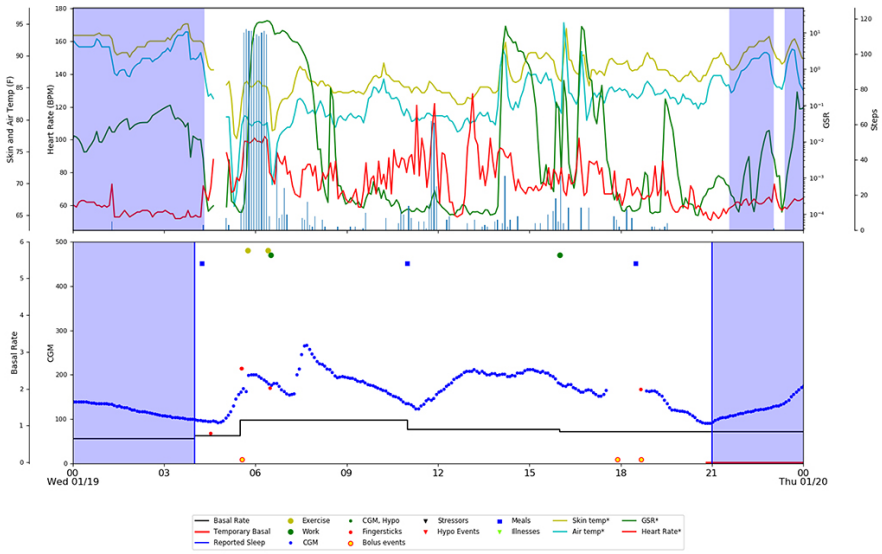

Figure 2: 24-hour measurements of one patient from the OhioT1DM Viewer [MB20].

2.3.3 MIMIC-IV:

The proposed model aims to generalize beyond diabetes forecasting to other medical applications, such as predicting disease progression in HFpEF patients. The MIMIC-III dataset [JPS+16] contains de-identified electronic health records (EHRs) of ICU patients, including vital signs (heart rate, blood pressure, oxygen saturation, etc.), medication records, and laboratory results. For this study, a subset of MIMIC-IV focusing on cardiovascular patients is utilized. The target variable, mortality risk, was divided into two groups: death within 30 days and death within one year. The exogenous variables include vital signs and laboratory values, while gender and comorbidities are used to split the data into multiple cohorts. By analysing the data in different cohorts, it is possible to get more specific and accurate counterfactual interventions.

2.3.3.1 Preprocessing

Following a preceding study[SBA+24], the International Classification of Diseases (ICD) codes were used for the initial preprocessing. The ICD-codes are a standardized international classification system used for the categorisation and encoding of diseases, symptoms, and associated health-related conditions. By using the appropriate ICD-9 and ICD-10 codes, as outlined in Table 1, the hospital admissions involving patients aged ≥ 18 with HFpEF as a primary diagnosis have been identified. Given that the diagnosis was based on ICD codes, the clinical notes were analysed in order to validate the selection of patients. This was achieved through filtering the clinical notes on mentions of the left ventricular ejection fraction (LVEF) value, with a value of 50 and above being counted as a normal LVEF value. Some clinical notes only mentioned a normal or preserved LVEF value with out a measured LVEF. These were also counted as normal LVEF values. Table 1 also shows the number of hospital admissions per diagnosis. The study sample consisted of 16122 individual hospitalizations with a suspected diagnosis of HFpEF. We had access to clinical notes for 11720 (72.7%) hospital admissions of which 4458 (38%) had an LVEF measurement reported. Of these, 3798 (85.2%) had an LVEF value $\geq 50\%$, and 400 (9%) had an LVEF $< 50\%$. An additional 260 (5.8%) admissions had mention of a normal or preserved LVEF. For these 4058 admissions, vital signs and laboratory values were available for 2432 (60%). It should be noted that in this instance, only the most recent admission of a patient who had previously been admitted with a similar diagnosis was taken into consideration. Prior admissions were incorporated into the analysis as a comorbidity, and after adding all laboratory values, vital signs and comorbidities, the resulting number of unique hospital admissions is 2113 with 1845 unique patients.
The extracted features are listed in table 2, split into four categories. These are the targets (Death within 30 days, Death within 1 year) as well as vital signs and laboratory values, comorbidities, and gender. Prior admission was included in the list of comorbidities, since it is here used as a comorbidity for the clustering and not the forecasting.

2.3.3.2 Clustering

The MIMIC data does not only include a wide range of features, but also a great number of comorbidities. Since these comorbidities can influence the chances of HFpEF, it is

Diagnosis	ICD Code	Frequency
Unspecified diastolic (congestive) heart failure	I5030	38
Diastolic heart failure, unspecified	42830	69
Acute diastolic (congestive) heart failure	I5031	84
Acute diastolic heart failure	42381	180
Chronic diastolic (congestive) heart failure	I5032	256
Chronic diastolic heart failure	42382	453
Acute on chronic diastolic (congestive) heart failure	I5033	426
Acute on chronic diastolic heart failure	42833	623

Table 1: The corresponding Diagnosis and ICD-9 and ICD-10 codes for HFpEF.

important to include these in the analysis. In this study, the comorbidities were used to cluster the patients, to get more specific counterfactuals. For this, the data was split according to patients having similar comorbidities to get factual cohorts. Another split was made by dividing the data on gender, since HFpEF is more prevalent in female patients and might need different treatment. Figure 3 shows the prevalence of different comorbidities of the MIMIC patients in the clusters, divided into four sub figures depending on the clustering coefficient and the gender. Figure 4 shows the Principal Component Analysis (PCA) of the different comorbidities, again divided into the same subgroups.

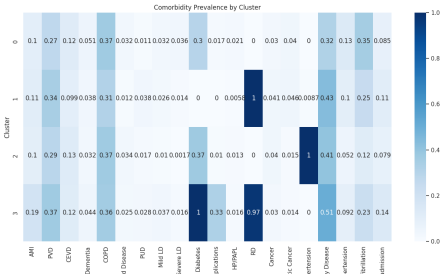

(a) Comorbidities in 4 clusters.

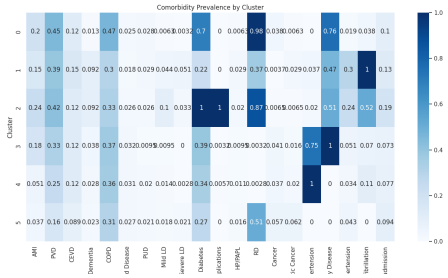

(b) Comorbidities in 6 clusters.

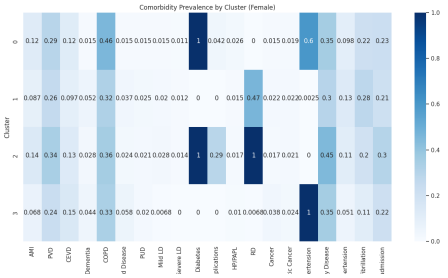

(c) Comorbidities for female patients in 4 clusters.

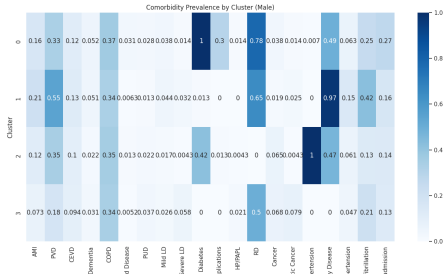

(d) Comorbidities for male patients in 4 clusters.

Figure 3: Prevalence of different comorbidities of the MIMIC patients in the clusters. There are 4 subgroups, clustering by comorbidity with $k = 4$, clustering by comorbidity with $k = 6$, clustering only the female patients with $k = 4$ and clustering only the male patients with $k = 4$.

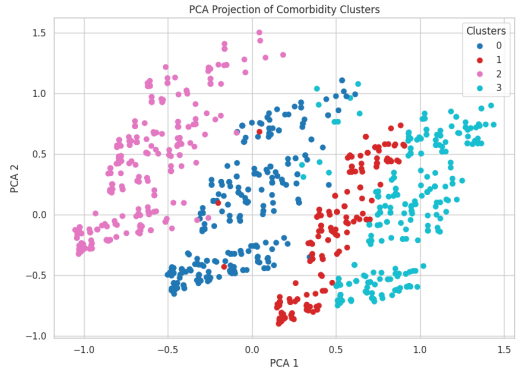

(a) PCA clustering in 4 clusters.

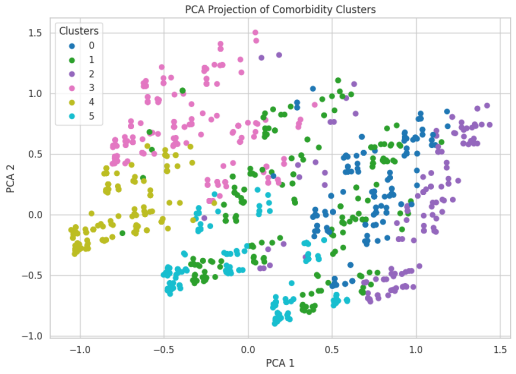

(b) PCA clustering in 6 clusters.

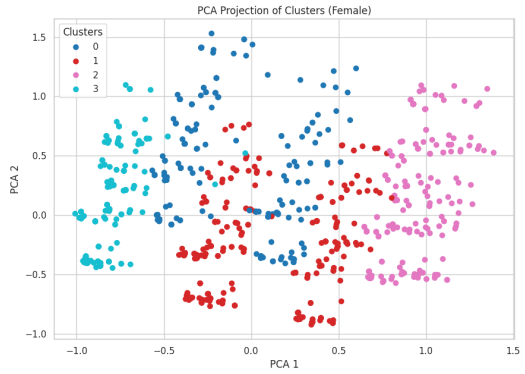

(c) PCA clustering for female patients in 4 clusters.

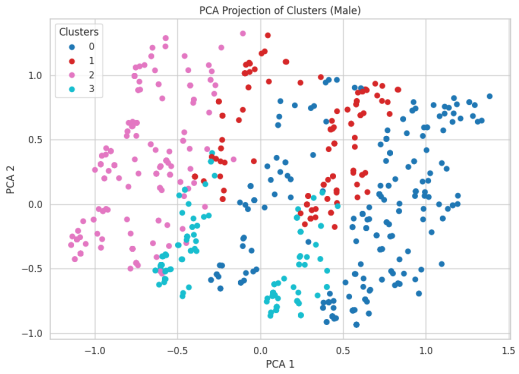

(d) PCA clustering for male patients in 4 clusters.

Figure 4: Principal component analysis (PCA) clustering of different comorbidities of the MIMIC patients. There are 4 subgroups, clustering by comorbidity with $k = 4$, clustering by comorbidity with $k = 6$, clustering only the female patients with $k = 4$ and clustering only the male patients with $k = 4$.

2.4 Experiments

2.4.1 Experimental Setup

The model can be split into two main parts. Initially a multivariate forecasting model is used to make a first forecast for both the target variable and the exogenous variables. This forecast is then used for the second part, where different regression models are used to change the exogenous and target variable to get the desired outcome. For the forecasting part we used GRU and NBEATS and for the second part we used four different models. Here the focus lies on using very different kinds of models, like a statistical (SARIMAX), a regression based (OLS), and two different deep learning based (GRU and NBEATSx) models.

2.4.1.1 Multivariate Forecasting:

For the multivariate forecasting, two main models have been used: (1) a 2-layer GRU model with 200 units at each layer and a linear output; and (2) a 4-layer NBEATS model with a forecast and backcast layer as well as a linear output. For both models early stopping with a patience of 10 epochs was applied to prevent over-fitting, with a fixed learning rate of 0.0001. For the forecasting tasks different back horizons and forecast windows were used and analysed. To evaluate the DL models two metrics were used: symmetric mean absolute percentage error (sMAPE) and root mean squared error (RMSE), where lower scores indicated a better predictive performance. The best performing model was then used for the counterfactual generation.
[**TODO:** Extend on method]

2.4.1.2 Counterfactual Generation:

For the counterfactual generation four different models have been used, all following a similar implementation. First two subsets of test samples were selected using two thresholds. This way, the samples were divided into a hyperglycemia set (blood glucose levels $\geq$ 180 mg/dL) and a hypoglycemia set (blood glucose levels $\leq$ 70 mg/dL) and then the following procedure was used:

- Bound Generation: Polynomial-based upper and lower bounds were generated for each test sample's predicted output, targeting desired glucose thresholds within a given window.
- Gradient Perturbation: For each forecasting model, the model was inverted by optimizing the exogenous inputs via gradient descent to steer the predicted output within the generated bounds.
- Loss Function: A custom loss function was used to penalize deviation from the bounds, and gradients were approximated using automatic differentiation or finite differences depending on model compatibility.

The models used for the counterfactual generation span both traditional statistical methods and deep learning architectures. [**TODO:** Extend on method, add more about mimic]

SARIMAX: The Seasonal Autoregressive Integrated Moving Average with Exogenous Variables (SARIMAX) model was employed to account for seasonality and external factors. Model parameters, including the order of autoregression (p), differencing (d), and moving average (q), were selected based on the Akaike Information Criterion (AIC). Exogenous inputs such as insulin dosage and carbohydrate intake were incorporated as regressors, and model parameters were optimized using maximum likelihood estimation.
OLS: Ordinary Least Squares (OLS) regression was used to examine linear relationships between exogenous variables and the target series. Feature engineering involved the creation of time-lagged variables and interaction terms between insulin and carbohydrate intake. To mitigate overfitting, regularization was applied. Additionally, linear constraints on exogenous variables were enforced post-hoc to facilitate counterfactual generation.
GRU: A Gated Recurrent Unit (GRU) network was implemented. The GRU architecture consisted of two layers, each with 128 hidden units, and dropout regularization set

at 0.2 to prevent overfitting. The network was trained using the Adam optimizer with an initial learning rate of 0.001, which was reduced by a factor of 0.1 if the validation loss plateaued over five epochs. Counterfactual explanations were generated by computing gradients of the output with respect to exogenous inputs, enabling identification of minimal interventions.
NBEATSx: The NBEATSx model was utilized, extending on the standard N-BEATS architecture by incorporating exogenous variables into its forecasting blocks. The model employed trend and seasonality decomposition through fully connected layers, and included exogenous inputs such as carbohydrate intake, insulin dosage, and physical activity. Quantile loss was used during training to capture distributional uncertainty, and feature importance analyses were performed to assess the contribution of exogenous variables to forecast accuracy.

2.4.2 Evaluation Metrics

[**TODO:** check, rewrite? unsure] To evaluate the quality of the counterfactual interventions, multiple evaluation metrics were implemented. First, traditional forecasting performance was measured using Root Mean Squared Error (RMSE) and Symmetric Mean Absolute Percentage Error (sMAPE), giving a quantitative assessment of prediction accuracy across the forecast horizon. For the evaluation of the generated counterfactuals, several additional metrics were introduced. These have been applied to ensure that the newly generated data for the exogenous variables is realistic, plausible and applicable.

RMSE, sMAPE scores sum of MSE scores, normalize for horizon?

Average value of change The average value of change quantifies the magnitude of adjustments made to the exogenous variables in order to achieve the desired forecasted outcome. For this the averaged original results of the multivariate forecast were compared to the averaged results of the counterfactual generation. euclidean distance?
The fraction of values to change captures the proportion of exogenous variable entries that required modification, offering insight into the sparsity of the interventions. By evaluating for how many of the timesteps in the time series the data changes, it is possible to analyse the differences that the counterfactuals
Severity of change To further characterize the nature of the interventions, the severity of change metric measures the relative intensity of the modifications compared to the original values. outlier score, LOF-score compare original exog to changed prediction
Fitting of predictions in bounds Additionally, the fitting of predictions within bounds was evaluated, reflecting the extent to which the counterfactual predictions adhered to the predefined upper and lower target constraints. This was done using the euclidean distance of the predicted target to the bounds. how good is the prediction, one in the band better than others?
Compare exogenous variables to those of a healthy patient Finally, to ensure the plausibility of the counterfactual scenarios, the modified exogenous variable profiles were compared to reference profiles from healthy patients. This comparison provides a qualitative and quantitative check on the biological or clinical realism of the generated counterfactual forecasts.
what are the differences in exog? changes from healthy patient

3 Results

3.1 Multivariate Forecasting

[**TODO:** explain chosen horizon, back horzion] To evaluate the performance of the multivariate forecasting and to ensure a realistic basis for the counterfactual generation, both the GRU and the N-BEATS model were tested across multiple datasets and forecasting configurations. The forecasting quality was assessed using two standard metrics: Symmetric Mean Absolute Percentage Error (sMAPE) and Root Mean Squared Error (RMSE). Models were trained on historical segments of the data and evaluated on subsequent future segments, allowing for a robust comparison between predicted and actual values. Table 3 summarizes the results across different datasets, prediction horizons, and back horizons. For the OhioT1DM dataset, N-BEATS consistently outperformed the GRU model in both sMAPE and RMSE across all configurations. Notably, with a back horizon of 12 and a forecast horizon of 6, N-BEATS achieved a sMAPE of 6.03 compared to GRU's 6.28, and a lower RMSE of 14.15 versus 14.85 for GRU. The same pattern was observed for back horizon 6 and 24, with N-BEATS slightly outperforming GRU in all cases. For the SimGlucose dataset, N-BEATS again generally showed improved forecasting performance. While GRU slightly outperformed N-BEATS in sMAPE for the 20-step back, 5-step horizon configuration (0.3792 vs. 0.3867), N-BEATS achieved a substantially lower RMSE (0.8271 vs. 1.6770), indicating more accurate absolute predictions. This performance gap widened in the 40-back, 10-horizon configuration, where N-BEATS clearly surpassed GRU on both metrics. [**TODO:** add mimic] Overall, these results demonstrate that the N-BEATS model generally offers superior performance across datasets and configurations, especially in terms of RMSE, making it a strong candidate for generating accurate multivariate forecasts and serving as a foundation for counterfactual analysis.

Table 3: Multivariate forecasting training metrics.

Dataset	Back Horizon	Horizon	Model	sMAPE	RMSE
OhioT1DM	12	6	GRU	6.2816	14.8471
			NBEATS	**6.0328**	**14.1500**
	24	6	GRU	6.1983	14.6856
			NBEATS	**5.8003**	**13.7677**
SimGlucose	20	5	GRU	0.3792	1.6770
			NBEATS	**0.3867**	**0.8271**
	40	10	GRU	1.5423	5.5572
			NBEATS	**1.4303**	**3.0461**
MIMIC			GRU		
			NBEATS		

[**TODO:** rerun, recalculate results] To complement the quantitative evaluation of the multivariate forecasting models, several visualizations were created to illustrate how well the N-BEATS and GRU models track actual future values. These plots compare the predicted time series against the true values for randomly selected test samples from the

datasets. Each subplot presents a single test sample, with time steps on the x-axis and the corresponding variable value on the y-axis. The actual values are shown in blue, while the predicted values are shown in orange. These plots offer a qualitative insight into the temporal alignment and amplitude accuracy of the forecasts, beyond what is captured by metrics like sMAPE or RMSE.

3.1.1 SimGlucose

For a back horizon of 20 timesteps and a horizon of 5 timesteps, both the GRU and N-BEATS models operate on a relatively short forecast horizon, making it easier to capture the trend with high fidelity. As shown in Figure 5, N-BEATS predictions closely align with the actual values across multiple samples, reflecting low forecasting error. Minor deviations appear mostly at the end of the forecast window. While the trend direction for the GRU predictions is usually correct, the model exhibits slightly larger prediction drift compared to N-BEATS, especially in sharper transitions. Still, GRU maintains reasonable short-term accuracy. For a back horizon of 40 timesteps and a horizon of 10 timesteps, the forecast horizon is increased, making the prediction task more difficult. Figure 6 shows the N-BEATS model's ability to handle long-range dependencies. Although small prediction lags and amplitude mismatches occur, the model captures the overall progression well, preserving directionality in most sequences. When looking at the GRU predictions under the same setup, the model struggles a bit more with extended forecasts, often showing divergence from actual trajectories, particularly toward the final time steps. These deviations are consistent with the slightly higher RMSE reported for this configuration.

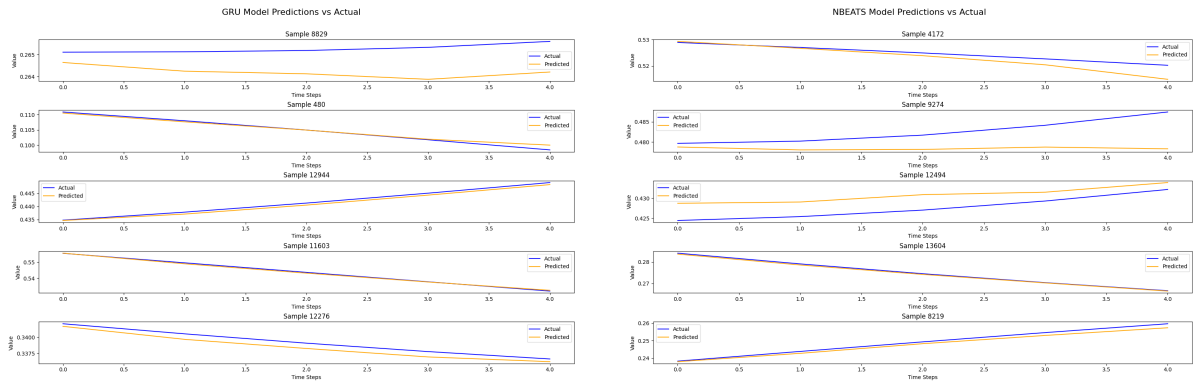

(a) Results of the multivariate forecasting using GRU.

(b) Results of the multivariate forecasting using NBEATS.

Figure 5: Results of the multivariate forecasting for the SimGlucose dataset with back horizon = 20 and forecast horizon = 5, showing the accuracy of the forecasting.

3.1.2 OhioT1DM

Figure 7 compare N-BEATS and GRU predictions for a back horizon of 12 timesteps and 6 future timesteps. The N-BEATS model tracks the general shape and scale of the actual values effectively. Although slight under- or over-predictions occur, especially in rising or falling trends, the model remains closely aligned overall. In contrast, the GRU predictions

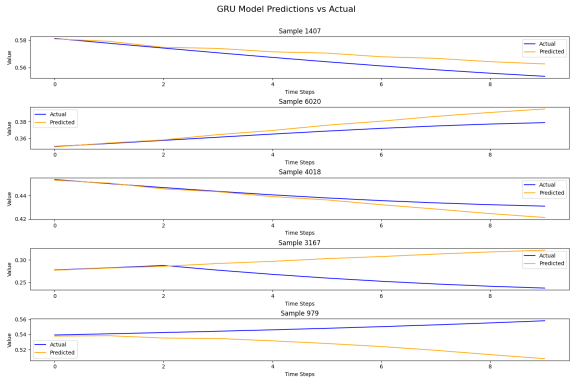

(a) Results of the multivariate forecasting using GRU.

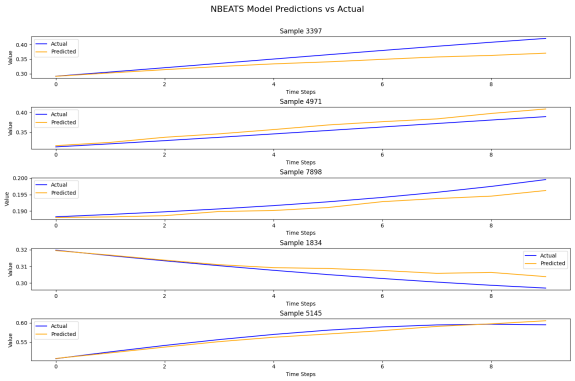

(b) Results of the multivariate forecasting using NBEATS.

Figure 6: Results of the multivariate forecasting for the SimGlucose dataset with back horizon = 40 and forecast horizon = 10, showing the accuracy of the forecasting.

tend to diverge slightly more in the later steps of the forecast horizon. GRU often preserves the direction of the trend but struggles with amplitude and slope consistency, leading to larger deviations as the prediction window progresses. With a back horizon of 24 timesteps and the same future timesteps, figure 8 depict the performance of N-BEATS and GRU under a longer input sequence. The figure illustrates that N-BEATS maintains robust trend prediction, with only modest lag or dampening effects in some samples. The model adapts well to both upward and downward trajectories. The GRU model performs more variably under this longer back horizon. While the general trajectory is still often captured, the forecasts occasionally overreact or smooth out variations, resulting in lower precision at the end of the forecast horizon.

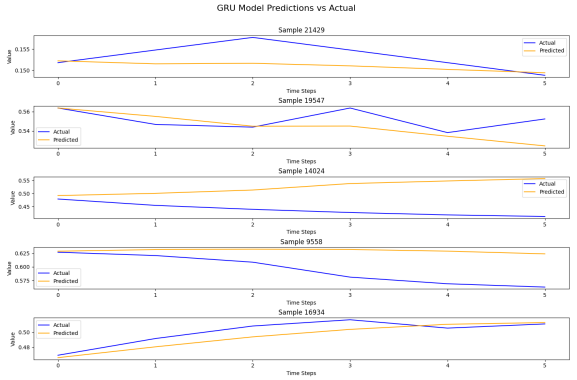

(a) Results of the multivariate forecasting using GRU.

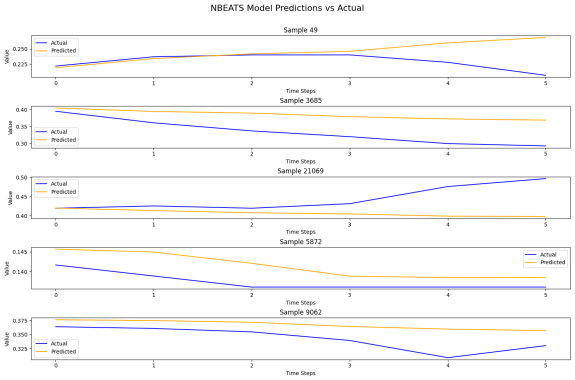

(b) Results of the multivariate forecasting using NBEATS.

Figure 7: Results of the multivariate forecasting for the OhioT1DM dataset with back horizon = 12 and forecast horizon = 6, showing the accuracy of the forecasting.

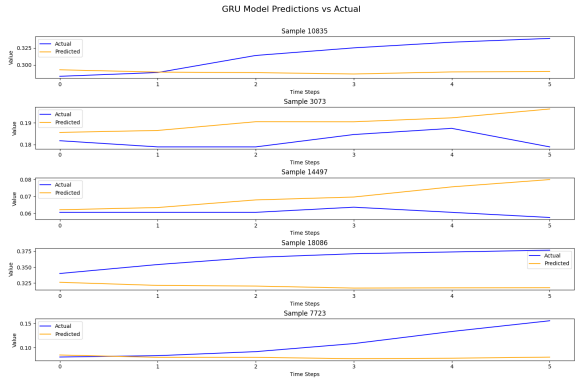

(a) Results of the multivariate forecasting using GRU.

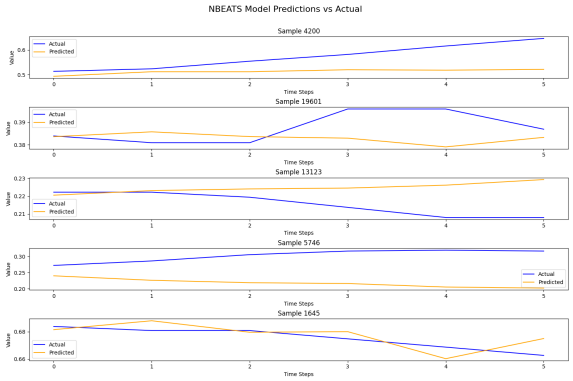

(b) Results of the multivariate forecasting using NBEATS.

Figure 8: Results of the multivariate forecasting for the OhioT1DM dataset with back horizon = 24 and forecast horizon = 6, showing the accuracy of the forecasting.

3.1.3 MIMIC

3.2 Counterfactuals

3.2.1 OhioT1DM

Figure 10 shows an example of the generated counterfactuals. It is a small sample of 6 timesteps, where the blood glucose level is aroung 155, which is lower than the original 180-190. This new BG level is within the calculated desired bounds. The generated exogenous variables differ a lot from the previous values, giving possible changes that might improve the blood glucose level.
To compare the newly generated exogenous variables to actual values, we found some examples in the data with a similar target to a newly predicted target. By comparing their exogenous variables, we can evaluate the realism of the generated counterfactuals. This is important to make sure that the counterfactuals are actionable and usable in the long run. For this, two samples of 6 timesteps with a minimal euclidean distance (2.0295) were found and its exogenous variables were compared. Figure **??**

3.2.2 SimGlucose

3.2.3 MIMIC

3.3 Measurements

3.3.1 Average value of change

Figure 11 shows two instances of the generated counterfactuals as well as the original exogenous data, using the OhioT1DM data.
Figure 12 shows the averaged absolute change between the original and generated time series of all four features of the OhioT1DM dataset.

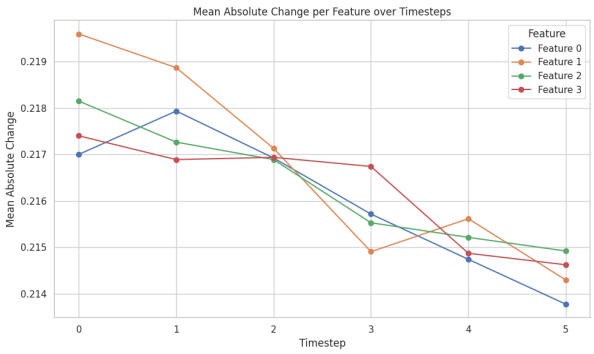

Figure 12: Caption

3.3.2 Coefficient of determination

3.3.3 Severity of change

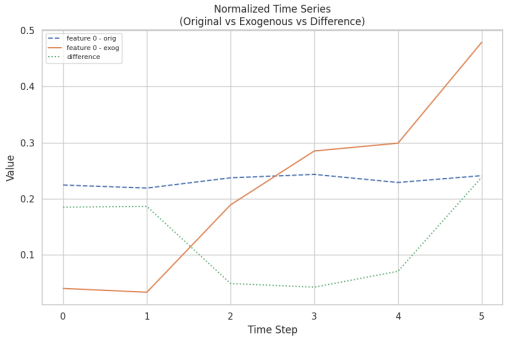

(a) Example 1

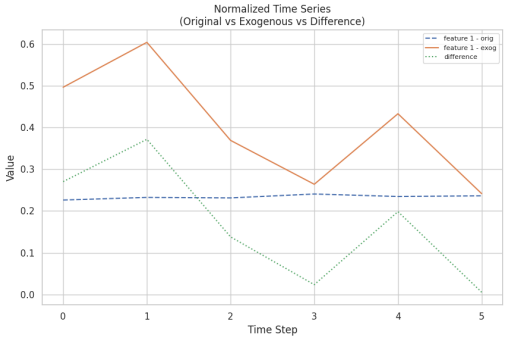

(b) Example 2

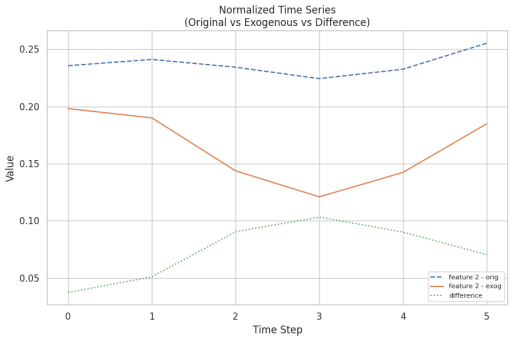

(c) Example 2

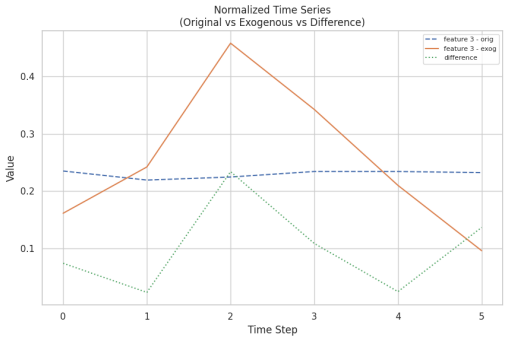

(d) Example 2

Figure 13: Visualization of the difference between the original exogenous variables and the generated counterfactuals as well as a measured distance per feature.

References

[AALC21] Emre Ates, Burak Aksar, Vitus J Leung, and Ayse K Coskun. Counterfactual explanations for multivariate time series. pages 1–8, 2021.

[ame25] 2. diagnosis and classification of diabetes: standards of care in diabetes—2025. *Diabetes Care*, 48(Supplement_1):S27–S49, 2025.

[ASFWHY+25] Nur Farah Afifah Ahmad Sukri, Wan Mohd Amir Fazamin Wan Hamzah, Mohd Kamir Yusof, Ismahafezi Ismail, Harmy Mohamed Yusoff, and Azliza Yacob. A systematic literature review on machine learning in healthcare prediction. *International Journal of Online & Biomedical Engineering*, 21(6), 2025.

[BAI25] Mamoune Benaida, Ibtissam Abnane, and Ali Idri. Deep learning based one step and multi-steps ahead forecasting blood glucose level. *Expert Syst. J. Knowl. Eng.*, 42(1), 2025.

[BP11] Barry A Borlaug and Walter J Paulus. Heart failure with preserved ejection fraction: pathophysiology, diagnosis, and treatment. *European heart journal*, 32(6):670–679, 2011.

[CHN+21] Ran Cui, Chirath Hettiarachchi, Christopher J Nolan, Elena Daskalaki, and Hanna Suominen. Personalised short-term glucose prediction via recurrent self-attention network. pages 154–159, 2021.

[Com25] American Diabetes Association Professional Practice Committee. 6. glycemic goals and hypoglycemia: Standards of care in diabetes—2025. *Diabetes Care*, 48(Supplement_1):S128–S145, 2025.

[Dia] Last Accessed: Jul. 5, 2025. Available: https://www.who.int/health-topics/diabetes.

[FAJ+18] Ian Fox, Lynn Ang, Mamta Jaiswal, Rodica Pop-Busui, and Jenna Wiens. Deep multi-output forecasting: Learning to accurately predict blood glucose trajectories. pages 1387–1395, 2018.

[GBV+24] Raffaele Giancotti, Pietro Bosoni, Patrizia Vizza, Giuseppe Tradigo, Agostino Gnasso, Pietro Hiram Guzzi, Riccardo Bellazzi, Concetta Irace, and Pierangelo Veltri. Forecasting glucose values for patients with type 1 diabetes using heart rate data. *Comput. Methods Programs Biomed.*, 257:108438, 2024.

[Gui24] Riccardo Guidotti. Counterfactual explanations and how to find them: literature review and benchmarking. *Data Mining and Knowledge Discovery*, 38(5):2770–2824, 2024.

[HMH+25] Yue Hu, Fanghui Ma, Mengjie Hu, Binbing Shi, Defeng Pan, and Jingjing Ren. Development and validation of a machine learning model to predict the risk of readmission within one year in hfpef patients: Short title: Prediction of hfpef readmission. *International Journal of Medical Informatics*, 194:105703, 2025.

[HSL+23] Chenlu Hong, Linjuan Sun, Guangwen Liu, Boyuan Guan, Chengfu Li, and Yanan Luo. Response of global health towards the challenges presented by population aging. *China CDC Weekly*, 5(39):884, 2023.

[HSYZ23] Jianing Hao, Qing Shi, Yilin Ye, and Wei Zeng. Timetuner: Diagnosing time representations for time-series forecasting with counterfactual explanations. *IEEE Transactions on Visualization and Computer Graphics*, 30(1):1183–1193, 2023.

[JHS+22] Mohd Javaid, Abid Haleem, Ravi Pratap Singh, Rajiv Suman, and Shanay Rab. Significance of machine learning in healthcare: Features, pillars and applications. *International Journal of Intelligent Networks*, 3:58–73, 2022.

[JPS+16] Alistair EW Johnson, Tom J Pollard, Lu Shen, Li-wei H Lehman, Mengling Feng, Mohammad Ghassemi, Benjamin Moody, Peter Szolovits, Leo Anthony Celi, and Roger G Mark. Mimic-iii, a freely accessible critical care database. *Scientific data*, 3(1):1–9, 2016.

[KBKB23] Pınar Özen Kavas, Mehmet Recep Bozkurt, İbrahim Kocayiğit, and Cahit Bilgin. Machine learning-based medical decision support system for diagnosing hfpef and hfref using ppg. *Biomedical Signal Processing and Control*, 79:104164, 2023.

[KCS+20] Shruti Kaushik, Abhinav Choudhury, Pankaj Kumar Sheron, Nataraj Dasgupta, Sayee Natarajan, Larry A Pickett, and Varun Dutt. Ai in healthcare: time-series forecasting using statistical, neural, and ensemble architectures. *Frontiers in big data*, 3:4, 2020.

[KM25] Deepjyoti Kalita and Khalid B. Mirza. Multivariate glucose forecasting using deep multihead attention layers inside neural basis expansion networks. *IEEE J. Biomed. Health Informatics*, 29(5):3654–3663, 2025.

[KS20] Zahra Karevan and Johan AK Suykens. Transductive lstm for time-series prediction: An application to weather forecasting. *Neural Networks*, 125:1–9, 2020.

[LBF13] Marco Lippi, Matteo Bertini, and Paolo Frasconi. Short-term traffic flow forecasting: An experimental comparison of time-series analysis and supervised learning. *IEEE Transactions on Intelligent Transportation Systems*, 14(2):871–882, 2013.

[LCP+25] Francisco J. Lara-Abelenda, David Chushig-Muzo, Pablo Peiro-Corbacho, Ana M. Wägner, Conceição Granja, and Cristina Soguero-Ruíz. Personalized glucose forecasting for people with type 1 diabetes using large language models. *Comput. Methods Programs Biomed.*, 265:108737, 2025.

[LH+24] Pei Hung Liao, Chung Lieh Hung, et al. Diagnostic yield and model prediction using wearable patch device in hfpef. In *Innovation in Applied Nursing Informatics*, pages 25–30. IOS Press, 2024.

[MB20] Cindy Marling and Razvan Bunescu. The ohiot1dm dataset for blood glucose level prediction: Update 2020. In *CEUR workshop proceedings*, volume 2675, page 71. NIH Public Access, 2020.

[MGL+20] Awais Malik, Gauravpal S Gill, Fahad K Lodhi, Lakshmi S Tummala, Steven N Singh, Charity J Morgan, Richard M Allman, Gregg C Fonarow, and Ali Ahmed. Prior heart failure hospitalization and outcomes in patients with heart failure with preserved and reduced ejection fraction. *The American journal of medicine*, 133(1):84–94, 2020.

[MKT+24] Kirsty McDowell, Toru Kondo, Atefeh Talebi, Ken Teh, Erasmus Bachus, Rudolf A De Boer, Ross T Campbell, Brian Claggett, Ashkay S Desai, Kieran F Docherty, et al. Prognostic models for mortality and morbidity in heart failure with preserved ejection fraction. *JAMA cardiology*, 9(5):457–465, 2024.

[MMA+21] Theresa A McDonagh, Marco Metra, Marianna Adamo, Roy S Gardner, Andreas Baumbach, Michael Böhm, Haran Burri, Javed Butler, Jelena Čelutkienė, Ovidiu Chioncel, et al. 2021 esc guidelines for the diagnosis and treatment of acute and chronic heart failure: Developed by the task force for the diagnosis and treatment of acute and chronic heart failure of the european society of cardiology (esc) with the special contribution of the heart failure association (hfa) of the esc. *European heart journal*, 42(36):3599–3726, 2021.

[MML+14] Chiara Dalla Man, Francesco Micheletto, Dayu Lv, Marc Breton, Boris Kovatchev, and Claudio Cobelli. The uva/padova type 1 diabetes simulator: new features. *Journal of diabetes science and technology*, 8(1):26–34, 2014.

[MPS19] Nishita Mehta, Anil Pandit, and Sharvari Shukla. Transforming healthcare with big data analytics and artificial intelligence: A systematic mapping study. *Journal of biomedical informatics*, 100:103311, 2019.

[MSG14] Prapanna Mondal, Labani Shit, and Saptarsi Goswami. Study of effectiveness of time series modeling (arima) in forecasting stock prices. *International Journal of Computer Science, Engineering and Applications*, 4(2):13, 2014.

[OHH+06] Theophilus E Owan, David O Hodge, Regina M Herges, Steven J Jacobsen, Veronique L Roger, and Margaret M Redfield. Trends in prevalence and outcome of heart failure with preserved ejection fraction. *New England Journal of Medicine*, 355(3):251–259, 2006.

[RCR23] Ignacio Rodríguez-Rodríguez, María Campo-Valera, and José-Víctor Rodríguez. Forecasting glycaemia for type 1 diabetes mellitus patients by means of iomt devices. *Internet Things*, 24:100945, 2023.

[RNZ17] Muhammad Imran Razzak, Saeeda Naz, and Ahmad Zaib. Deep learning for medical image processing: Overview, challenges and the future. *Classification in BioApps: Automation of decision making*, pages 323–350, 2017.

[SBA+24] Ikgyu Shin, Nilay Bhatt, Alaa Alashi, Keervani Kandala, and Karthik Murugiah. Predicting 30-day and 1-year mortality in heart failure with preserved ejection fraction (hfpef). *medRxiv*, 2024.

[SK25a] Yiheng Shen and Samantha Kleinberg. Personalized blood glucose forecasting from limited CGM data using incrementally retrained LSTM. *IEEE Trans. Biomed. Eng.*, 72(4):1266–1277, 2025.

[SK25b] Yuyang Sun and Panagiotis Kosmas. Integrating bayesian approaches and expert knowledge for forecasting continuous glucose monitoring values in type 2 diabetes mellitus. *IEEE J. Biomed. Health Informatics*, 29(2):1419–1432, 2025.

[VDH21] Sahil Verma, John Dickerson, and Keegan Hines. Counterfactual explanations for machine learning: Challenges revisited. *arXiv preprint arXiv:2106.07756*, 2021.

[WMSP23] Zhendong Wang, Ioanna Miliou, Isak Samsten, and Panagiotis Papapetrou. Counterfactual explanations for time series forecasting. In *2023 IEEE International Conference on Data Mining (ICDM)*, pages 1391–1396. IEEE, 2023.

[WSMP24] Zhendong Wang, Isak Samsten, Ioanna Miliou, and Panagiotis Papapetrou. Comet: Constrained counterfactual explanations for patient glucose multivariate forecasting. In *2024 IEEE 37th International Symposium on Computer-Based Medical Systems (CBMS)*, pages 502–507. IEEE, 2024.

[Xie18] Jinyu Xie. Simglucose v0.2.1. https://github.com/jxx123/simglucose, 2018.

[ZGW+21] Liye Zhou, Zhifei Guo, Bijue Wang, Yongqing Wu, Zhi Li, Hongmei Yao, Ruiling Fang, Haitao Yang, Hongyan Cao, and Yuehua Cui. Risk prediction in patients with heart failure with preserved ejection fraction using gene expression data and machine learning. *Frontiers in genetics*, 12:652315, 2021.

[ZLH+18] Taiyu Zhu, Kezhi Li, Pau Herrero, Jianwei Chen, and Pantelis Georgiou. A deep learning algorithm for personalized blood glucose prediction. pages 64–78, 2018.

Feature types	Specifics	Occurrences
Targets		
	Death within 30 days	136
	Death within 1 year	150
Vital signs and laboratory values		
	BMI	1845
	Heart Rate	1845
	SpO2	1845
	Diastolic BP	1837
	Systolic BP	1837
	Temperature	1829
	Creatinine	1825
	Sodium	1825
	Bicarbonate	1823
	Hemoglobin	1814
	WBC Count	1814
	Platelet Count	1812
	Troponin	958
	NT-proBNP	76
Comorbidities		
	Diabetes	798
	RD	768
	Coronary Artery Disease	761
	COPD	658
	Hypertension	599
	PVD	577
	Atrial Fibrillation	424
	AMI	230
	CEVD	218
	Prior Admission	188
	Pulmonary Hypertension	170
	Diabetes + Complications	156
	Dementia	75
	Cancer	65
	Metastatic Cancer	50
	Rheumatoid Disease	50
	Mild LD	46
	PUD	40
	Moderate/Severe LD	30
	HP/PAPL	27
Gender		
	Male	773
	Female	1072

Table 2: All features of the MIMIC data divided by feature types: Target, Vital signs and laboratory values, Comorbidities, and Gender.

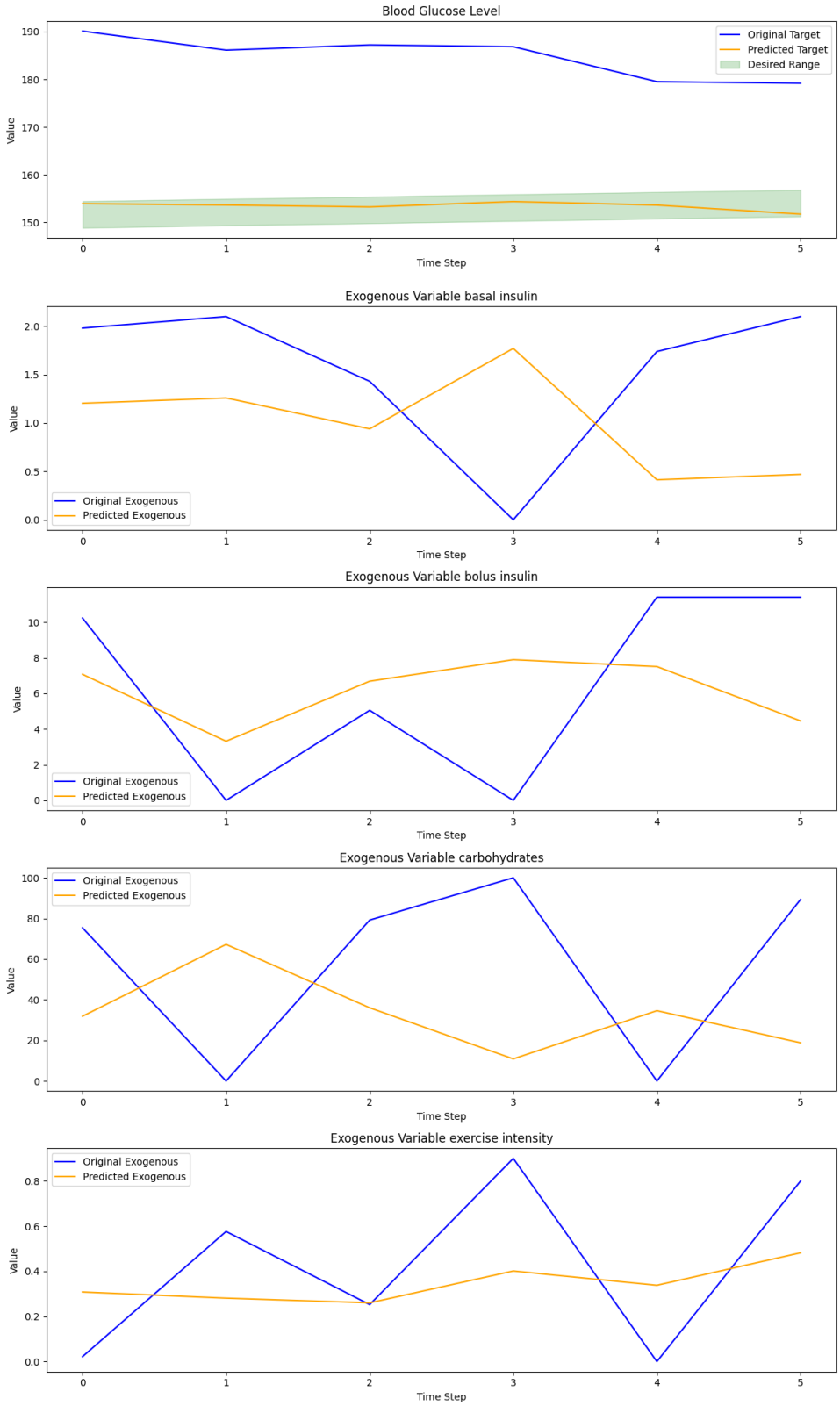

Figure 9: Example of the generated counterfactuals, with the blood glucose level within the desired bounds. The different exogenous variables, with the original values in blue and the predicted in orange.

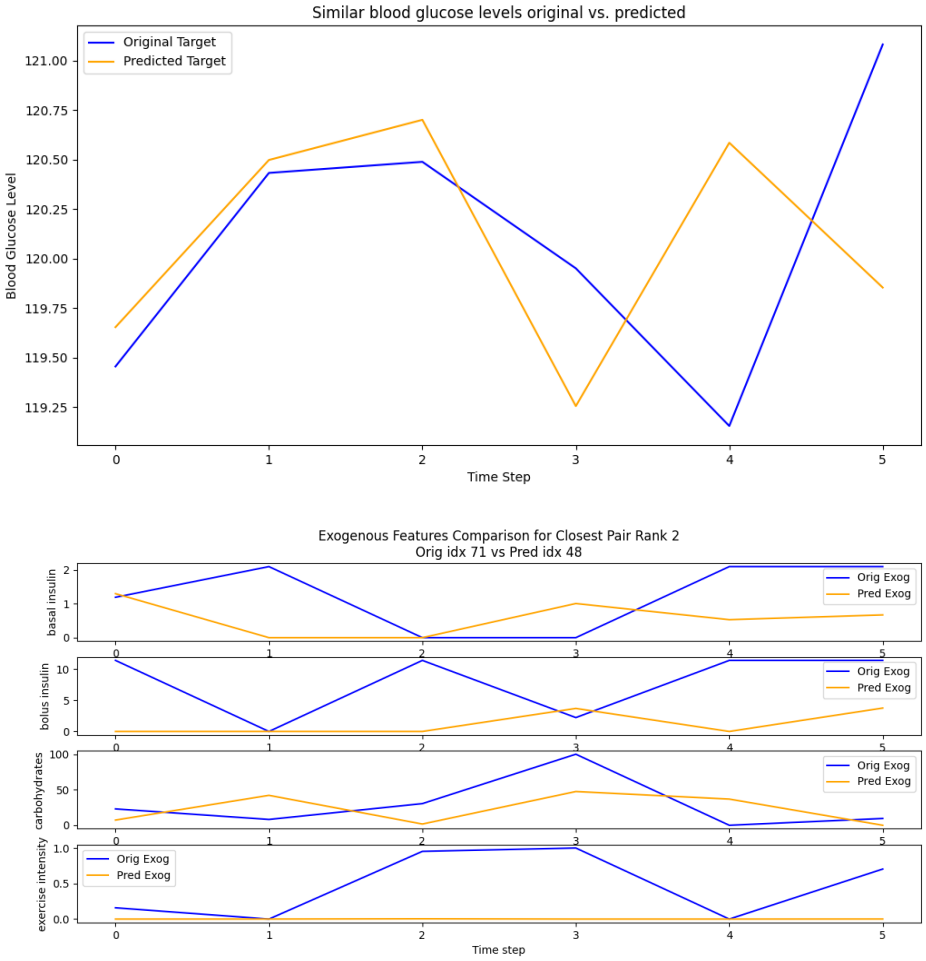

Figure 10: Two samples with a similar blood glucose level.

Feature	Pair 71, 48		Pair 27, 82		Pair 27, 11		Pair 68, 31		Pair 74, 75	
	Act	Norm	Act	Norm	Act	Norm	Act	Norm	Act	Norm
Basal Insulin	2.1575	0.5678	3.1525	0.6280	2.0002	0.2891	2.7798	0.3388	2.9895	0.5143
Bolus Insulin	19.4057	0.5012	21.2238	0.8798	19.8393	0.4116	10.8953	0.2978	15.0757	0.3838
Carbohydrates	100.5660	0.4907	80.1914	0.5888	125.0327	0.4353	31.7565	0.4943	143.2101	0.5476
Exercise Intensity	1.1705	0.5956	1.5558	0.9469	1.1187	0.5106	0.9448	0.2775	0.8671	0.7661

Table 4: Euclidean distances between original and predicted exogenous features for the 5 closest target pairs, with both actual and normalized values.

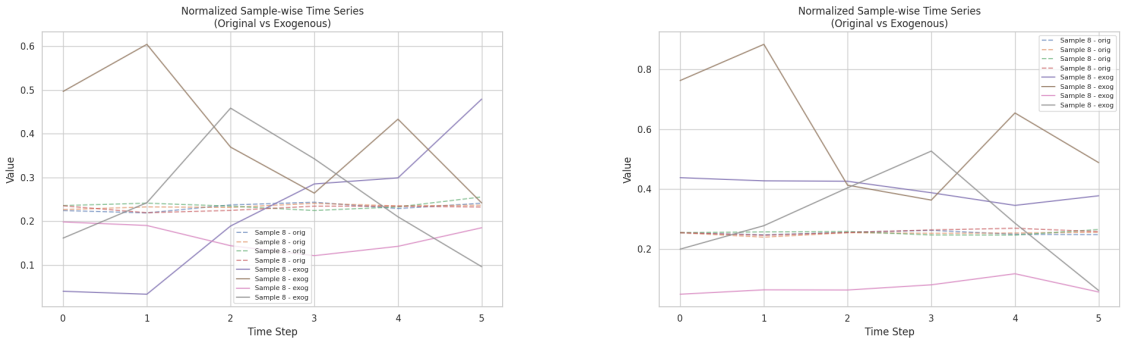

(a) Example 1

(b) Example 2

Figure 11: Two examples of the difference between the original exogenous variables and the generated counterfactuals.